Implementation of Electric Field Integration Equation in Parallel Mode for A Terrain Profile

By

Saubhagya Sharma

Dissertation

Submitted to the

Trinity College Dublin, University of Dublin

in fulfilment of the requirements for the Degree of

Master of Science in Computer Science (Future Networked System)

Declaration

I, the undersigned, declare that this work has not previously been submitted as an exercise for a degree at this, or any other University, and that unless otherwise stated, is my own work.

Saubhagya Sharma

Trinity College Dublin

August 2022

Permission to Lend and/or Copy

I, the undersigned, agree that Trinity College Library may lend or copy this thesis upon request.

Saubhagya Sharma

Trinity College Dublin

August 2022

Implementation of Electric Field Integration Equation in Parallel Mode for A Terrain Profile

Abstract

The study is based on parallel methods for computations of electric field magnitudes in a terrain profile. The Electric Field Integration Equation is one of the numerous approaches used to predict how communication signals will propagate, along with ray tracing and integral methods (EFIE). It was able to compute the electric field E that an electric current J creates because the EFIE established a relationship. There is a terrain profile and the formula established is E=ZJ. In light of this, the objective of this project is to find workable solutions that will hasten the graphic determination of the signal coverage for each terrain profile. The parallelization approach, which is a more effective method of doing this, is hereby presented. This method uses split terrain groups and segments for computation. Up to 700 meters from the transmitter, calculations are performed. Groups and n-arbitrary segments are further split into the terrain profile. Both propagation and dispersion occur between each segment and the transmitter. The electric field is simultaneously and calculated in parallel. This method is found to be at least 2000 times faster than the traditional EFIE method.

Acknowledgments

I would like to thank several people who helped me to make this thesis accomplishment possible. First and foremost, I would like to express my gratitude to my supervisor Prof. Dr. Eamonn O'Nuallain. His painstaking guidance and supervision over the last year for the thesis helped me achieve close to what I had targeted at the onset of the project. Sincere thank also goes to Professor Donal O'Mahony, my co-supervisor for his special feedbacks.

I am thankful to the staffs in Trinity College Library for the easy access to all the books and resource materials that were required for the thesis.

Further, I would also like to thank the college administrator and School of Statistics and Computer Science, Trinity College coordinators for maintaining an atmosphere in the labs and libraries where we could work and brainstorm peacefully.

A huge and special mention to my classmate Boshi Pan with whom I navigated through as we were both under a common supervisor.

-Saubhagya Sharma

Contents

List Of Figures

Chapter 1: Introduction

This chapter serves as an introduction to the project and goes through its motivation, goals, and anticipated outcomes. Finally, there is the discussion of this document's structure.

1.1 Background

The Electric Field Integration Equation is one of the many methods in order to calculate the mode of propagation of communication signals ranging from ray tracing to integral methods. The EFIE established a relationship thereby allowing the calculation of an electric field E which is produced by an electric current (J). There is the equation E=ZJ and a terrain profile. The signal coverage over the terrain span for 700 metres is observed using the mathematical equations proposed in (Nuallain, 2008).

Making some few approximations in the beginning makes it easier to find the solution. The first is that it is started off by assuming that every bit of radiation originating transmitters is mirrored by the surfaces we're thinking about. These surfaces could be metropolitan areas, steep terrain, or rolling farmland - all of them using a digital terrain map to define (DTM). The PEC Model refers to this simplification. PEC, or "perfect electrical conductor," stands for this. As a result, they are incapable of resisting the electrical current flow. Metals are decent conductors but not flawless ones. This close estimate is suitable for land-based emitters where the radiation's angle of incidence approaches $\pi/2$ High frequencies and radians are used. According to the second approximation, all energy promulgates away and is connected to the first. the way of the transmitter. The Forward Scattering Approximation is the name of this approximation. For both approximations, some radiation will in fact pass through the surface and There will be some radiation that returns to the transmitter. But for most of you, it is adequate to use these two approximations. When a transmitter's radiation "hits" a surface, it induces (or "causes") an electric current to flow. flow over that area. The next step is to designate the letter "J" for this surface current. Then, this current radiates again. to every other point on the surface, as well as to every point above it. When it spreads to other people subsequently, similar to the field incidental from of the source, it as creates an electric field at certain prevailing at the time.

When a transmitter's radiation "hits" a surface, it induces (or "causes") an electric current to flow. flow over that area. Further, the letter "J" is designated for this surface current. Then, this current radiates again. to every other point on the surface, as well as to every point above it. When it spreads to other people subsequently, similar to the field incidental from of the source, it as creates an electric field at certain prevailing at the time.

$$E(r) = \frac{\beta\eta}{4} \int_S J(r') H_0^{(2)}(\beta | r - r' |) dr'.$$

Where,

r : Vector whose end-point is the scattering point

r': Vector whose endpoint is the receiving point

E(r) : The source electric field incident on the surface at a point by r

ŋ: wave impedance of the medium through which the radiation propagates

$H_0^{(2)}$: Zero order Hankel function (Nuallain, 2008)

It is necessary to perform this equation's numerical solution using a computer because there isn't an explicit solution for J(r)'. The other quantities E(r), $\frac{\beta\eta}{4}$, S and $H_0^{(2)}(\beta|r - r'|)$ are the values which have been estimated already beforehand. The electric field as from source (transmitter) that is incidental on the surface at a point designated by the vector r is referred to as E(r). The observation point, or r, in this instance is on the surface.

In mathematics, with reference to the above equation $dx \rightarrow \Delta x$ and $\int \rightarrow \sum$ The above equation is now as shown.

For each point j then, the following system of simultaneous equations are obtained:

$$E^{Inc}(r) = \frac{\beta\eta}{4}\int_S J(r')H_0^{(2)}(\beta\,|\,r-r'|)dr'$$

$$E_j = \sum_{i=1}^{i\le N} J_i Z_{ij} \qquad \text{for } j = 1....N$$

$$E_j = E(r_j) = H_0^{(2)}(\beta|r_j|)$$
$$Z_{ij} \approx \Delta s\frac{\beta\eta}{4}H_0^{(2)}(\beta\,|\,r_i - r_j\,|)$$
$$Z_{ii} \approx \Delta s\frac{\beta\eta}{4}\left(1 - j\frac{2}{\pi}\ln\left(\frac{1.781\beta\Delta s}{4e}\right)\right)$$
$$J_i = J(r_i)$$

$$\begin{aligned}
E_1 &= J_1Z_{11} + J_2Z_{21} + J_3Z_{31} + J_4Z_{41} \quad \cdots \quad J_NZ_{N1}\\
E_2 &= J_1Z_{12} + J_2Z_{22} + J_3Z_{32} + J_4Z_{42} \quad \cdots \quad J_NZ_{N2}\\
E_3 &= J_1Z_{13} + J_2Z_{23} + J_3Z_{33} + J_4Z_{43} \quad \cdots \quad J_NZ_{N3}\\
&\vdots \qquad\qquad\qquad\qquad\qquad\qquad\quad \vdots\\
E_N &= J_1Z_{1N} + J_2Z_{2N} + J_3Z_{3N} + J_4Z_{4N} \quad \cdots \quad J_NZ_{NN}
\end{aligned}$$

The term Zii is called the 'self-term'. $JiZii$ represents the field scattered from point i to itself

Here there are N equations with N unknowns (J) which means it can be solved for J.. This can be written more compactly as a matrix equation:

$$\mathbf{E = ZJ}$$

E and J are N-dimensional column vectors. The impedance matrix Z is symmetric and N X N-dimensional. The components of Z's strictly lower and strictly higher triangles, respectively, correspond to forward and backscattering, respectively. a sampling periods.

1.3 Motivation

The major motivation of this research is to find effective measures which will make it faster to find the signal coverage for any terrain profile and position of a transmitter graphically. For this a faster and effective method, called the parallelization method is presented in addition to another faster method done, whereby computation is done on terrain groups and segments bifurcated.

Further, this can open better doors and more effective research into the cognitive radio technology. For each transmission request, cognitive radios (CRs) examine a supporting network architecture. By determining the anticipated impact of the transmission on entrants and other CR devices from the CR's geo-location and antenna attributes, the network server either approves or denies these requests. Therefore, effective knowledge of electric field and current coverage will make the picture clearer and jobs easier.

1.4 Hypothesis

Coding the equations in 1.1 and mathematics in MATLAB for a terrain profile and transmitter takes a long time to execute and examine the signal coverage and propagation loss. This study seeks to find effective measures which will make it faster to find the signal coverage graphically. For this a faster and effective method, called the parallelization method is presented in addition to another faster method done, whereby computation is done on divided terrain profile groups and segments.

The use of this equation in MATLAB coding into a terrain profile data-set is made. The model that is used (parallelization method) is to be faster in execution than the traditional Electric Field Integration Equation model with the same/similar output.

1.5 Document Structure

The state of the art in EFIE and parallelization interface with relation to signal loss and fading is introduced in Chapter 2. The design of our methodology is outlined in Chapter 3. In Chapter 4, the section looks at how the code was put into practice. In Chapter 5, the findings from the test is assessed in details. In Chapter 6, the conclusion is done by providing a summary of the project and the participation.

Chapter 2: State of Art

The goals of the research, the driving forces behind it, and the methodology were all introduced in Chapter 1. In this chapter, the context of the study and assess the current state of electrical field integral equations and parallelization solving research is looked at.

2.1 State of the Art

Fading in wireless communications is the fluctuation of a signal's attenuation due to numerous factors. These parameters include the date, the location, and the radio frequency. Large-scale fading and small-scale fading are the two main categories of fading.

2.1.1 Small Scale Fading

The topic means the term used to describe abrupt variations in a radio signal's amplitude and phase across a short distance or in a small space of time (on the order of seconds) (a few wavelengths). At the time the receiver is relocated with just some small portion of a wavelength, the immediate received radio power may change by much as 30 to 40 dB due to small-scale fading. Each route will have its one Doppler shift, lag of time, plus the impedance of path in a dynamic working milieu, and multipath transmission produces a moment signal as the mobile changes position. Such a network is time-varying but linear. Because there are several forms of the transmitted that arrive at random intervals, this particular fading is often termed as Rayleigh fading. In the absence of a no-line-of-sight (NLOS) component, a Rayleigh distribution statistically describes the received signal's envelope. A Rician distribution will then be used to explain unless there is a LOS component.

Since many cognition properties that are intensive of computation can be implemented at the side of the network, the demands on cognitive radio user tools can be greatly alleviated with powerful support in the side. The effort on a single user's paraphernalia can be reduced and the cognitive radio adaption process sped up by collaborative and distributed data and further processed data processing across the network. Given the numerous restrictions placed on price-sensitive use, such

as low power devices, signal processing ability, and memory footprint, this is a crucial tactic to aid in the commercialization of cognitive radio technology. (El-Gohnary, 2011)

A. **Fast Fading** is mostly caused by reflections from the surface and transmitter or movement of the receiver. When that signal bandwidth is equal to or greater than the Doppler bandwidth and the channel variations are equal to or greater than the signal variations, high doppler spread is seen. It produces Inter Symbol Interference and linear distortions in the baseband signal's form (ISI). Adaptive equalization is one method for getting rid of ISI.
B. **Slow Fading:** The main cause of it is shadowing, which happens when tall buildings or other geographical features block the LOS. Sluggish fading exhibits minimal doppler spread because the channel fluctuations are slow in comparison to the signal variations and the doppler bandwidth is smaller than the frequency of the signal. It causes a decrease in SNR, which can be remedied by applying receiver diversity and error correction techniques.
C. **Multipath Fading:** If a signal reaches the receiver via multiple paths, causes it to happen. All frequency ranges, from lower frequencies to the microwave and bigger, are likely to be impacted by multipath fading. It causes phase aberrations and ISI by affecting the signal's amplitude along with the phase. There are two ways that multipath fading might impact signal transmission:
    i) Flat fading: All frequency components are basically impacted equally in flat fading. Over time, the amplitude changes as a result of flat multipath fading.
    ii) Selective Fading: Selective Fading, also known as Selective Frequency Fading, is what is multipath fading that is occured when the selected frequency component of the signal is impacted. That is a denotation of certain resonance frequencies of the same signal will exhibit higher error along with attenuation than other frequency components. Techniques like OFDM, which distributes the data from across spectral analysis of the signal to minimize data loss, can be used to address this.

2.1.2 Large Scale Fading

There is a continuous loss of power over a very long distance (a few hundreds or thousands thousand meters), and large-scale fading can be defined as the mean signal degradation, or the path loss caused by the movement over huge distances. It is influenced by the topography between both the transmitter and receiver. The power swings around an average value over such a distance, and

these variations have a fairly long period, according to analysis of the power about such a distance. An estimation of propagation loss taking it as function of the distance can be obtained from the parameters of large-scale fading, which are expressed in the terms of a percent of waste (nth - law) in addition to a sign allocated variability in and around the mean. (Ashikhmin, et al., 2018)

The Electric Field Integral Equation (EFIE) serves as one of the solutions to calculate the large-scale signal fading. The most important concept here being path loss. Every particular electromagnetic wave experiences a decrease in power density as it travels across space, which is defined as path loss (or path reduction). Path loss can be caused by a variety of things, such as the radio wave's natural expansion, a barrier causing diffraction path loss, or the existence of a material that blocks electromagnetic radiation. It is crucial to remember that even in cases of path loss, the broadcast signal may still take additional routes to reach its target location; this is referred to as multipath. Since various waves of transmitted data follow different routes, the wave may recombine at the destination, resulting in wildly different received signals.

The surroundings of the sender and receiver have a direct impact on path loss. In order to create path loss models, a combination of computational techniques and approximations based on empirical measurements from channel sounding tests is used. Propagation route loss often increases with frequency and distance.

$$P_l = 10 \log_{10} \left(\frac{16\pi^2 d^n}{\lambda^2} \right)$$

Where P_l is the calculated path loss, d means the gap between the propagation, n denoting that path loss exponent varying between two and the λ is the free space wavelength.

2.1.3 Maxwell’s Equations

The results of Maxwell's equations can be used to anticipate the existence of electromagnetic waves that are propagating [Maxwell, 1865]. The relationships established in the fluctuations of vector geomagnetic H and also the specific vector applied electric E in time and space are described by

these equations. inside of a medium. The E field is produced by and usually expressed per meter. either a free charge or a magnetic field that changes over time. The amperes per square meter of the H field meter and is produced by either a current or an electric field which alters as time passes. Four Maxwell's Equations are overall summed up as follows in words:

A magnetic field that changes over time generates an electric field. A current or an electric field with time-varying characteristics creates a magnetic field. Field lines may be continuous or may begin and end on charges. Continuous magnetic field lines exist. (Fette, 2006)

The very first two of the equations, known as Maxwell's curl (equations), have proportionality constants that determine the intensities of the fields. These are the medium μ permeability in henrys per meter and the media ε permittivity in farads per meter. Normally, they are stated in relation to the quantities in empty space:

$$\mu = \mu_0 \mu_r$$
$$\varepsilon = \varepsilon_0 \varepsilon_r$$

Where μ_o and ε_o are the free space values, found by:

$$\mu_0 = 4\pi \times 10^{-7}\ \mathrm{H\,m^{-1}}$$
$$\varepsilon_0 = 8.854 \times 10^{-12} \approx \frac{10^{-9}}{36\pi}\mathrm{F\,m^{-1}}$$

The same figures could be utilised as proper estimates in vapourless air at average pressure and temperature, however free space strictly refers to a vacuum.

2.1.4 Field Relationships

The electric field is expressed as,

$$\mathbf{E} = E_0 \cos(\omega t - kz)\hat{\mathbf{x}}$$

Where,

E_0 - field amplitude

ω - angular frequency in radians for a frequency f, value equivalent to 2 X 22/7 X Frequency

t – time elapsed

k – Wavenumber (m^{-1})

z – Distance alongside z-axis

x – Component vector alongside the positive x-axis

The distance across where the phase of the wave is changed by 2π radians is denoted by the wavelength λ. Hence,

$$k = \frac{2\pi}{\lambda}$$

Likewise, the magnetic-field vector H is also expressed as,

H = $H_0\cos(\omega t - kz)\hat{y}$

H_0 – Amplitude of magnetic field

$\hat{y}$ – The Unit vector in north y-axis

This brings us to the concept of wave impedance. The equations discussed above align with Maxwell's equations if and only if ratio of the amplitude of fields remain unaltered in a particular medium.

$$\frac{|\mathbf{E}|}{|\mathbf{H}|} = \frac{E_x}{H_y} = \frac{E_0}{H_0} = \sqrt{\frac{\mu}{\varepsilon}} = Z$$

where Z is measured in ohms and is known as the wave impedance.

In a free space, keeping μ_r and ε_r as 1, the wave impedance is,

$$Z = Z_0 = \sqrt{\frac{\mu_0}{\varepsilon_0}} \approx \sqrt{4\pi \times 10^{-7} \times \frac{36\pi}{10^{-9}}} = 120\pi \approx 377\Omega$$

So, to define the entire field for a plane wave in a free-space along with some other even medium, that makes it enough to provide a given field quantity along with Z.

The phase velocity 'v' about which wave moves in the 'S' direction, or the velocity of an unit with fixed phase on the wave, is given by

$$v = \frac{\omega}{k} = \frac{1}{\sqrt{\mu\varepsilon}}$$

Here, the wavelength (λ) = $\frac{v}{f}$

Another similar topic is the lossy medium. When the medium is particularly conductive, the wave's amplitude decreases as it travels farther into the medium as the wave's energy is extracted and transformed into heat.

Now the following can be written,

$$\mathbf{E} = E_0 \exp[j(\omega t - kz) - \alpha z]\hat{\mathbf{x}}$$

And,

$$\mathbf{H} = H_0 \exp[j(\omega t - kz) - \alpha z]\hat{\mathbf{y}}$$

The α is also referred to as the attenuation constant and is expressed in terms of per metre [m-1] unit, depending on the permittivity, permeability , wave frequency, and conduction potential of the medium, σ, expressed in per-ohm-metre [Ω-1]. The fundamental variables of the medium are known as σ, μ, and ε together.

When a result, as the wave moves through the medium, the field intensity (including electric and magnetic) decreases exponentially.

Also rough surface scattering also needs to be understood here. Specular reflection is the result of the reflection processes that have only been relevant to smooth surfaces up to this point. The reflected wave scatters from numerous locations on the surface as the surface becomes more rougher, expanding the scattered energy. As a result, there is less energy radiated in the convex direction and more energy is radiated in other dimensions. The amount of scattering is influenced by the angle of incidence and the surface irregularity in relation to the wavelength. As the incidence

angle approaches graze incidence and as the wavelength is increased, the surface's perceived roughness decreases.

The scattering problem is modelled using a variety of mathematical methods. Popular approximations include Born or distorted-Born methods, perturbation theory, and the Kirchhoff approximation. They are rather easy to execute even though they have a limited amount of validity. Rigid, accurate approaches have taken centre stage as computing power has improved. Integral equations are the most widely used of these, therefore this overview is limited to these and a few approximations. Even with this limitation, there are several varieties and various approaches to solving the problem of cognitive radio.

A transceiver can proactively determine which exchanges are in use and which ones are not in cognitive radio (CR), a form of wireless communication. The transceiver then immediately switches to open channels, avoiding busy ones. These features aid in the radio frequency (RF) spectrum's best possible utilisation. It lessens user interference overall. Additionally, it boosts spectrum efficiency and enhances consumers' quality of service (QoS) by avoiding occupied channels.

The RF Remote spectrum is a fixed resource which is often distributed via licensing. The Federal Communications Commission (FCC) as well as the National Telecommunications and Information Administration are jointly in charge of it in the United States (NTIA). (Fette, 2006)

2.1.5 Radio Environment Mapping

Next is the concept of Radion Environment Mapping.

The network support for cognitive radio is divided into two groups, internal networking capabilities and the external network support, from the perspective of the user of the cognitive radio. The radio channel that the CR is connected to is referred to as the internal network. The internal network can offer a variety of communication functions as well as some cognitive functionality. The cognitive radio network, for instance, can identify the neighbourhood’s other users' usage patterns and offer location data and site-based essential services to the user.

The progress of wireless networks from legacy transmitters up to the cognitive radio networks and also from the cohabitation of several fragmented radio channels to united network architectures depends largely on network support. Network-enabled cognitive radio, as described in this chapter, works in conjunction, regulator, and wireless carrier with the greatest amount of flexibility by establishing dynamic strategies on spectrum availability and accessibility.

For example, the information gathering for CR networks could be done by a distinct sensor network. An obsolete network or other cognitive radio channels could make up the external network. Externally and internally networks can work together to develop the REM and contribute in several ways. To take an instance, the global positioning system (GPS) or internal support via a positioning approach on the basis of the network can both be used to collect the location data required for a cognitive radio in interior even outside settings, respectively.

A network support tool which is utilised for the purpose of cognitive radio is basically called the radio environment map (REM). The radio ecosystem of cognitive radios is described by the REM, an approximation of real-world radio situations, in a number of different areas, including topographic maps, legal and policy frameworks, radio device capability profiles, and radio waves (RF) emissions. Even when the subscriber unit is rather basic, the REM, which is effectively an integrated spatial database, could be used to assist the cognitive works of the devices, like situation awareness (SA), argumentation, learning, and planning. The ARM, that is intended to be a genuine map of the entire set of radio activity in that infrastructure for the CR applications in unregulated large networks, can also be seen as an extension to the REM (UWANs).

Most cognitive functions in the CRN could be accomplished in a cost-effective manner because to the REM's ability to offer both current and historical radio environment information. Cognitive radios may do spectrum sensing using past information by utilizing the REM as opposed to continuously blindly scanning the entire spectrum. As a result, the radio front-observation end's time and energy usage can be greatly decreased. By loosening the limitations on broadcast power, contrast ratio, and sensitivities of the device, collaborative information processing approaches can further lower the expenses of a CR network.

The REM has a significant part in the cognitive radio run. The global or local REM can be influenced by both direct radio observations and information learned from network assistance. The

radio can be aware of its surroundings through visual examination, such as sensing of spectrum, or through REM. The cognitive radio uses reasoning and learning to recognize the radio scenario, gain knowledge from prior work and observations, to create judgments and plans to achieve its objectives. Once an activity is conducted or slated by that radio, the global REM and/or the localized REM must be refreshed to keep the information current.

The REM supports intelligent network functions by offering perceptive tactics to the network radio means management for legacy or hardware reconfigurable radios. The REM aids a cognitive radio in being aware of situations and making the best modifications in accordance with its goals. The REM is clear to the particular radio access technology (RAT) for the purpose of using, independent of whether the subscriber radio is cognitive or not, in a similar way to how a city map is instructive to every tourist whether they are taking the bus or driving a car. A radio can learn metrics of performance, application, topological, and network or routing information, and also the information about the MAC and physical (PHY) levels of communication packs, with the aid of the REM, in a variety of radio contexts. For instance, dependability and security are crucial if the radio is being used in a combat zone. Algorithms for frequency planning, encryption, anti-jamming coding scheme, specific source coding, and routing could all be used in this way. The REM can handle a variety of network designs, including point-to-point communications and dispersed, heterogeneous, or centralized networks. Additionally, it can facilitate cooperative information processing between several nodes for full awareness.

For a cognitive engine to use, the REM delivers extensive system-level knowledge. The cognitive engine, that forms the cognitive radio's core, is often designed as a software application with learning and memory components adaption methods. A cognitive network's decision-making process uses information stored in the REM, which is effectively a database. As a result, to build the cognitive network, numerous components are required in addition to REM. These components are made up of those decision, rational, and the cognition algorithms. The ability to distinguish the learning, reasoning, and decision-making processes from REM makes it possible to create a system that can handle a wide range of radio kinds, networks, and applications. (Saunders & Zavala, 2007)

To entirely utilize the REM to obtain SA and to facilitate self-learning, making of decision, and reasoning, AI approaches are helpful. For instance, a cognitive radio will score higher than those who do not if it learns to predict the location and chances of a spectrum hole or congestion arising.

It makes sense to give the CR some baseline knowledge in addition to the capacity to learn, just as advancement gives living organisms sufficient in-built impulses to allow them to live long enough to understand for themselves. The behaviour of the CRNS could become functionally independent of its prior knowledge after accumulating enough experience in its environment. When learning is considered, it is possible to create cognitive radios that work well in a wide range of settings.

The REM is thus an integrated database made up of information from various domains, including geographic attributes, services that are offered, spectrum laws, radio location and use, user and/or the service provider policies, along with prior understanding. A cognitive engine is capable to make use of a REM to improve or achieve most cognitive functions, including learning, reasoning, organizing, in addition to the predictive modelling. Using global and local REMs to use both public and private network support offers a practical strategy to develop cognitive radios that is dependable, adaptable, and economical. The network assistance can significantly reduce the demands over a cognitive structure thereby leading to an increase the overall dependability of the cognitive radio network. Given that spectral control and operation policy are dynamic, the in the sense that it enables flexibility and futureproofing, REM-based cognitive radio justification for authorities or providers to adjust their guidelines by appropriately updating the REMs. Due of the REM's extensive database, a less dearly, moderate radio component can is capable to achieve the fundamental cognitive capabilities required for cognitive radios by in relation to REM.

Since it is the system-level CR solution, the REM not just makes cognitive functions practical, but also more crucially, enables wireless communication networks evolve and converge with cost-effective databases. From remnant radio to the CR, the REM shows a seamless evolutionary path. The radio resource management (RRM) practiced in modern commercial wireless networks can also be seen as a natural but significant evolution. In order to provide for the heterogeneous cognitive wireless networking, the REM further possesses a significant potential for connecting/converging various wireless communication channels. This will enable the implementation of multiple network architectures on the radio and other technologies of access, such as WLAN, wireless personal area network (abbreviated as WPAN), Worldwide Interoperability for Microwave Access (also known as WiMAX), Beyond 3G(B3G), as well as the four-G systems.

A few significant unanswered questions are:

1. Could the local or global REM retain the accuracy of its data?

2. How up-to-date and granularly detailed must the data in the global and local REMs be for it to deliver the necessary execution?

3. What extent to more operating expense is required to maintain the REM, and can the users determine the limit of the network latency?

4. How successfully is to possible that an ad hoc mesh network be served by distributed local REMs?

5. How can the REM's reliability, security, privacy, and integrity be guaranteed?

The integration of the Okumura model with the entire lines of the terrain profile set was attempted but unfortunately due to time constraints, all the results could not be obtained. However, there are interesting observations as the formulae for suburban and metropolitan surfaces in regard to path loss were different from each other.

2.2 Literature Review

The research is based on an Integral Equation based propagation method presented in Centre for Telecommunications Value Chain Research (CTVR), Trinity College Dublin by Prof. Dr. Eamonn O Nuallain. (Nuallain, 2008). The "Hidden Node Problem" and how it can be solved using this technology and a Radio Environment Mapping server are both discussed. Concerns of importance for Cognitive Radio (CR) in terms of security and dependability real-time, accurate quantification of the effects of CR transmissions, assuaging the valid worries of Primary Users with relation to the application of CR technology. a plan for the propagating technique is developed in such a way that it is possible to fulfil execution times and accuracy requirements.

Prof. Dr. Eamonn O'Nuallain and team also undertook research regarding the parallel implementation of the EFIE. Researchers and engineers may now use effective and potent calculation methods, particularly when it comes to radiation and scattering issues, thanks to advancements in the IT sector. The EFIE algorithm, which calculates the surface current, is the subject of this paper's attempt to increase the effectiveness of the algorithm. (Delaney, et al., 2011)

A new way to speed up the computation of EFIE and the field which is near or to far-field translation in source renovation methods is put forth in a work by Rezvan Rafiee Alavi, et al. The ideal count of quadrature points for precise outcomes is determined by this procedure. The location of such points along with the accompanying weights then are determined theoretically as shuttered equations in a representation of a matrix, motivated by an adaptive implementation. In order to use the derived expressions as an analytical lookup table for entirely all triangles in the discrete - time mesh, those vertices could simply be fed in them. Iterative methods' lengthy processing times and inherent inaccuracy in polynomial-based Gaussian quadrature’s are avoided by this method. (Alavi, et al., 2020)

The stability of marching-on-in-time (MOT) solvers applicable to the study of smattering from self-supporting, 3-dimensional perfect electrically conducting (PEC) surfaces depends on the accurate estimation of the MOT matrix rudiments produced by a Galerkin discretization of a underlying integral equation, according to theoretical studies and practical experience. Unfortunately, using numerical methods to accurately evaluate the required 4-dimensional spatial integrals is too costly. The technique undertakes the use of Rao-Wilton-Glisson (RWG) geographic base functions and

Lagrange polynomial sequential growths, and it uses 2D integrals across the source coordinates which are assessed mathematically when the residual 2D integration placed above a testing coordinate is carried out numerically. The MOT solver was demonstrated to be reliable for a variety of situations with up to 50,000-time steps. (Shi, et al., 2010).

Diancheng Si and company conducted another study relevant to this on their paper for the IEEE Transactions on Instrumentation and Measurement journal. Solving data equations is now a challenge for the technique of determining the voltages of communication lines with the help of the nonlinear equations of the discussed electric field. In order to address the aforementioned issues, a method is provided that reduces transmission line voltage by positional applied electric integration based on D-dot sensors. Here in the context of the study, the transmitting wire power is effectively explained along with the Gauss-Legendre(G-L) mathematical optimization algorithm while using the floor as the enhanced capabilities and the perpendicular distance of the power line to the base akin to the path of the integral. A D-dot applied electric sensor is used to determine the immediate applied electric numbers with many endpoints on the integral path. The electric field dispersion data on the integration route produced by model is used to validate the G-L algorithm. Additionally, by improving the integral interval to make the location of the nodes of integral more logical, the G-L method has been improved. Finally, the LabVIEW-based measurement system is designed, and the analogue transmission line experiment platform is built. The results of the experiments demonstrate that the modified Gauss-Legendre algorithm which is on the basis of the D-dot sensor has a good precision with an error of the less than 1% for the measurement of transmission wire voltage. (Si, et al., 2019)

The wireless link environment often places limitations on telecommunications systems. The expected characteristics of a wired route are different from those of a wireless channel, which is unexpected. In fact, a combination in both the propagation loss factor (m) with free space fading channels that vary with surroundings was devised to get a more genuine condition of said path loss pattern. The main goal of this investigation is to increase staff awareness of these aspects and their influences while also imparting knowledge of the variables that impact generic path loss models. In a study by Tahreer Mohammad and team (Mahmood, et al., 2021), they categorize the variables into three groups: frequencies, various antenna strengths, and path loss coefficient.

MATLAB software has been used to model and examine these elements' effectiveness. The findings indicate that decreasing the antenna yields from 1 up until 0.25 units can result in a path loss increase of 1 dB, plus that when coefficient of the path loss (m) is put at 5, the loss reaches 120 dB and only considers for about 800 meters of sent signals when blocked in a structure. However, the route loss exceeds 85 dB contributes for over 800m of sent signals with the LOS setup (m = 1.6) in the building. What been found is the path losing performance is heavily affected by means of the frequencies and path loss exponent. The differing antenna increases can, however, possess a negligible impact in the performance. Through the use of path loss propagation models, this study aims to explain how each of these factors affects the receiver and the transmitter in order to assist the researcher and reader in making improvements or coming up with new ideas.

Another study of interest was (Kayode, et al., 2016)The ability to estimate the signal strength that will be received at a specific place is crucial for evaluating the total efficiency of just about any wireless system. The propagation loss in between the base stations and upwardly mobile user will determine this prediction. Due to significant inaccuracy brought on by greater carrier frequency and distance, few of the prevailing propagation route loss simulations, including Okumura, Free Space, Okumura-Hata, Davidson-Hata and Cost231 Hata, do not render suitable for forecasting of Long Term Evolution signal in the place Lagos. Therefore, these models must be optimized for compatibility with Lagos, Nigeria's LTE signal. This study examines the Okumura-Hata model's applicability to LTE signals. The drive test is used to determine the average radio strengths for three LTE sites in Lagos at various places. It is done to analyse the Okumura-Hata model and compare the results to the measured values. Least Squares is then used to optimize Okumura-Hata. Root Mean Square (RMS) error, a gauge of the performance of the model, is used to calculate that path loss. The outcomes demonstrate that now the RMSE is decreased between 13.46 all the way down to 0.63. This demonstrates the enhanced model's ability to forecast route loss with an accuracy of five percent and how it has has been demonstrated. The improved Okumura-Hata model values can therefore be used to estimate the transmission loss of LTE the place, as they hold conformity with or greater than the assessed data.

2.3 Summary

The EFIE, faster methods, signal loss, fading which are all the relevant fields of study and vital to this project have been introduced. There are several steps as well as equations to the methodologies that should be taken into account during the use of the given approaches.

Chapter 3: Design

In this section, the methodologies, approaches and all the events leading to the implementation and evaluation are discussed.

3.1 Tools Used

3.1.1 MATLAB

Engineers and researchers can use the programming environment MATLAB to study, create, and test systems and technologies for their work. The language used in MATLAB is a matrix-based and it enables the natural expression of computer calculation, is the core of MATLAB. For a variety of applications in industries and universities, including machine learning and artificial intelligence, signal processing as well as communications, computer vision, control mechanisms, telecommunications equipment, combinatorics, and computational biology, gazillions of engineers and independent researchers use MATLAB. It facilitates data analysis, algorithm development, model development, and application creation. Thus, it is an ideal choice for the project. To perform the simulations concurrently, MATLAB's 'parsim' function is used. To reduce overall simulation duration, the function spreads several simulations to multicore CPUs. In order to free up our time to work, 'parsim' also automates the establishment of parallel pools, locates file dependencies, and maintains build artifacts. Simulations in parallel can be run interactively or in batches.

3.1.2 Terrain Profile

Cutting transversely through the lines of a topographic map yields a topographic profile, also known as a topographic cut, which represents the relief of the terrain. The terrain profile has a mountainous feature. It was provided by the supervisor.

3.1.4 Base Papers

Much part of the study is based on the research paper 'A Proposed Propagation-based Methodology with which to address the Hidden Node Problem and Security/Reliability Issues in Cognitive Radio' published in 2008 in IEEE by Prof. Dr. Eamonn O Nuallain.

3.2 Implementation

Over the Terrain that spans 700 meters, the permeability of the medium is defined and the permittivity of the medium. Frequency of the signal that is 970 megahertz. Because here the quarter wavelength concept is used as the quarter of the wavelength is sufficient to calculate the information contained by the signal. The location parameter of the transmitter is also defined.

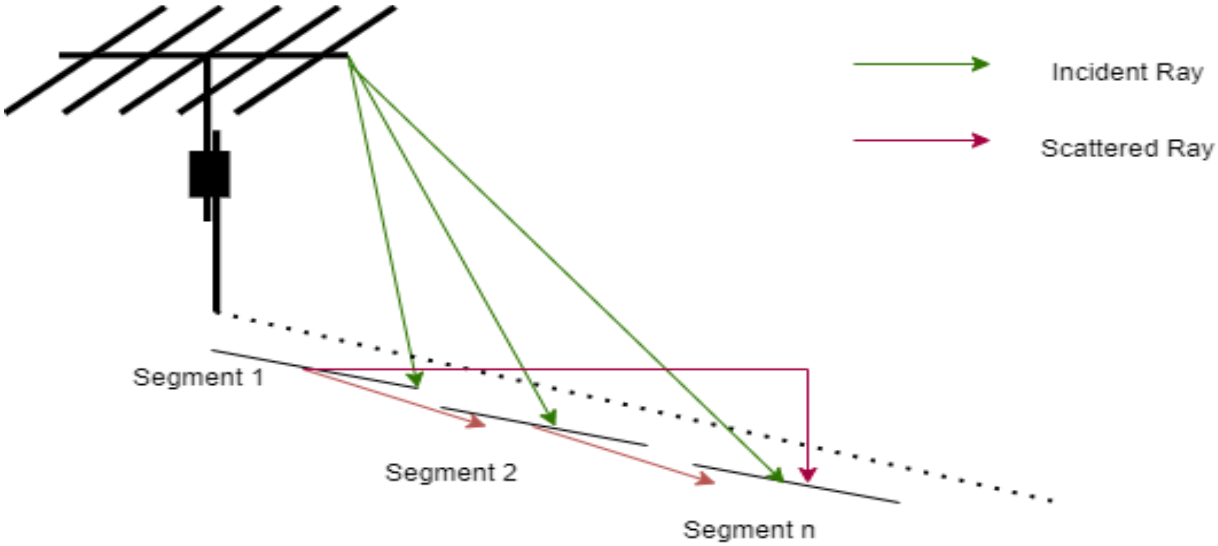

Figure 1 Parallelization Segmentation

Here the X defines the X coordinate. Y defines the Y coordinate and height of the source is defined by Y coordinate minus Terran height that is 390 as per the terrain file. Then the blank matrix is defined, a blank map. Here considers the group size of the segments is considered of about 13, and which and as per the terrain file, the lines of code are considering the step of the 10 segments. So finally, it is being defined in the equation. The Terrian length is the total length of 700 meter defined, so the code will have to calculate the total number of groups because the. Electric field and surface current will be calculated in terms of the per group, so. Next step is to calculate the total number of groups in our 700 length Tarrant 700-meter length talents that is calculated in the code. Here the quarter wavelength concept is also calculated because as said above, the quarter wavelength is sufficient enough to catch the whole signal. Hence, with this formula. Then the thing to do is to calculate the total number of groups which will be considered in the calculation. The self-impedance of the environment is then defined. It is self-impedance. It is a complex value. Basically, the standard value is considered to be 1.0 for the real part and 1.05 as the one for the

imaginary part. It is a consolidated value which is considered for the environment and impedance. Now it's time to calculate the surface current and electric field. So first the space to store the value of the surface current and electric field is made. Therefore, the blank matrix where the value of the surface current will be stored is defined. Initially, the 0 X 0 in this matrix is put. So here the matrix of the size zero is made. The electric field is expressed in terms of the decibel value. Again, the process is to create a blank matrix of the size zero that is a zero matrix of the same size.

And again, for the absolute value of the surface current, which is essential for our project, the calculation presents the results of the surface current in terms of the complex value. Now it is a must to calculate the absolute value to create the plot. So here the code converts that complex value in terms of the absolute. Then the next step is to create a blank matrix to store the absolute value of the surface current. And finally, this is the only space creation about the electric field and surface current. As the signal is an electromagnetic signal, it is a complex signal, so it is essential to calculate the Bessel function to calculate the value of this signal.

The Bessel function for this group size is calculated. And again, the constant value which is arrived from the vessel function and impedance value that is the self-impedance value of the environment. Now it's time to calculate the surface current value, so surface current value will be calculated for the whole total number of groups that are about 696. So, it is considered here as the code is initializing this loop for from the one and total number of groups plus one here, so a total of 697 for the 697 groups. Then the code calculates the surface current value as it is taken into account that there are the incident ray and also the ones scattered into it from previous segments. Basically, it is almost like the code summons propagating from each of the segments as well. Then the value of the surface current for each group is calculated. Each and every group with the specified formula mentioned above in the background gets the values, and finally stores the whole value in the surface Similarly, to calculate the electric field with the for the same number of groups, there is also initiation of a for loop. This whole for loop basically calculates the value of the electric field by the formula defined in the base paper. To perform the simulations concurrently, MATLAB's ‘parsim’ function is used. To reduce overall simulation duration, the function spreads several simulations to multicore CPUs. In order to free up our time to work, ‘parsim’ also automates the establishment of parallel pools, locates file dependencies, and maintains build artifacts. Simulations in parallel can be run interactively or in batches.

```
for n = 1:tot_groups+1
    electric_field(n) = Ei_Rad(bt * R_source_obs(n, qw, y));

    for m = 95:(n-1)
        electric_field(n) = electric_field(n) - const * surface_current(m) * H02(bt *
R_surface_obs(m, n, qw, y));

    end
    ef_db(n,1) = X(n, qw);

    ef_db(n,2) = 10 * log10(abs(electric_field(n))/sqrt(R_source_obs(n+1, qw, y)));

end

in = ef_db %Data storage of electric field.


%Model parallel simulation
for i = 700:-1:1:
    in(i) = Simulink.SimulationInput('fileID'); %Reloading Terrain Profile

    in(i) = in(i).setVariable('FeedTemp0', electric_field(i));
end
out = parsim(in, 'ShowProgress', 'on')
```

So, with the help of that formula, the electric field and store the value of the electric field, that is, that is in the form of the complex numbers is calculated. Electric field data is converted in terms of the DB decibel value, so it is converted in the decibel value by the equation. So finally, the electric field in terms of the decibel is defined. Now it is important to calculate both the surface current and electric field by the specified formulas. Now it's time to plot that data of the electric field and surface current with respect to the Terrain, so. To plot the graph. for the electric field, the plot command is created, and it is for the electric field versus the 700-meter span.

It will plot the value of the electric field with respect to the terrain of the 700 span and similarly. As stated earlier, to plot the data, the absolute value of the data is required. So, the surface current is calculated in terms of the complex value. Hence, first the code has to convert this complex value into the absolute form so the for loop initiated for the surface current calculated in the form of the

complex number is first converted in the absolute form, so surface absolute current basically defines the surface current in the absolute form and this data will be utilized to create the plot with respect to the. Now there are some functions which are utilized to calculate the space curve, surface current and. Electric field. The Hankel function is calculated, which is used to calculate the Bessel function for the complex signal, and similarly and there is a function for the electric field Bessel function utilized. To calculate the electric field, here there is another function. This function is utilised time and again. In terms of the quarter wavelength value of the signal, a there is a wide data. It is at some height from the ground, so it is the height is basically defined by the Y coordinate with respect to the ground height and it is also calculated in terms of the quarter wavelength data. So, some specified function is used to calculate. The signal traveling with respect to the height of the source. So, this function basically calculates the data of the signal traveling from the Y heighted source. These are also some data to calculate at the horizontal and the distance of the observation point from the source. Where the surface current and electric field to be calculated, it is also a specified function to calculate the distance between the surface to the observation point also. This function basically calculates the distance between the two points. Say suppose there are the suppose it is considered that the first effect at the one point and then effect on the other point so that those two points are to estimate how much height and how much away they are from each other. This function is basically calculating the distance between those two points. Z-self is basically. The impedance. It is a generalized value of the impedance. So, with the help of this impedance value and the beta value and quarter wavelength value, the Bessel function is calculated, and it is utilized. There is a function that basically defines the calculation of the Bessel function which is utilized to calculate the Hankel function.

Chapter 4: Evaluation

In this section the results and presented and evaluated. The comparison and contrast of the results from the original Electric Field Integral Equation with that of the one obtained from the parallelization method is also done.

4.1 EFIE Method Result

When plotting the electric magnetic field in Y-Axis against the distance in X-Axis using the above equations, the following graph is obtained. As it can be seen, as the distance approaches 700 metres the trough comes all the way down only to rise back. This is because of the nature of the Terrain Data set. This is the ideal graph that is obtained, and the study will be basing yhr research on this particular graph. The aim is to get it done in a matter of seconds and get a graph almost as close to the one below. As it is seen, for the first 100 metres (or 90 metres to be close), the graph has a regular rise and fall. After 300 metres up until 500 metres the trough comes all the way down finally hitting the bottom at the latter. This is because some of the trough lies in the Non-line-of-sight (NLOS) signal propagation state, so radiation creeps away. Then the trough rises back to a little less than the smallest positive value as the terrain span ends.

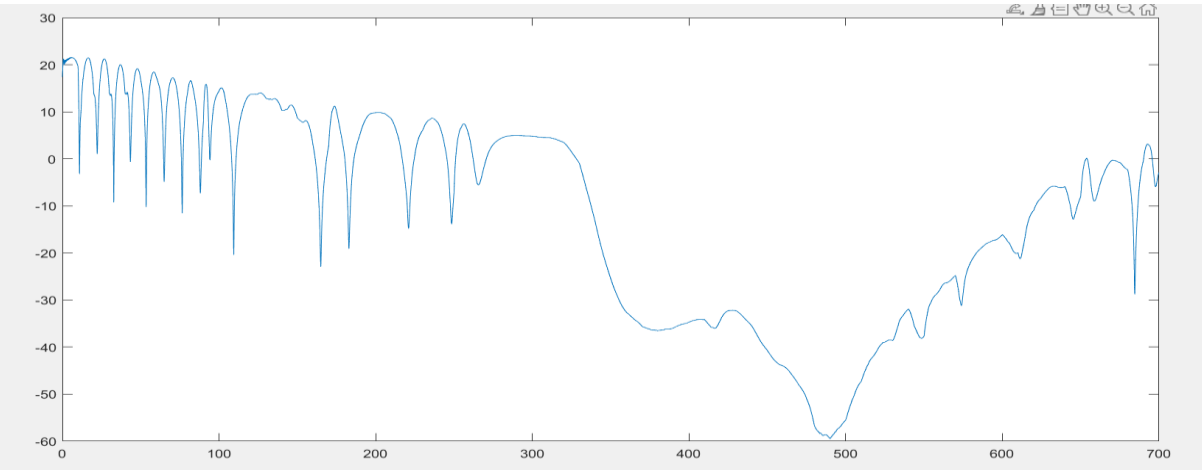

Figure 2 Graph of E vs Distance from Traditional EFIE

The following is the plot for the causing electric surface current. It is obvious that the current declines, stabilises at 350-550 metres and goes a little up there after.

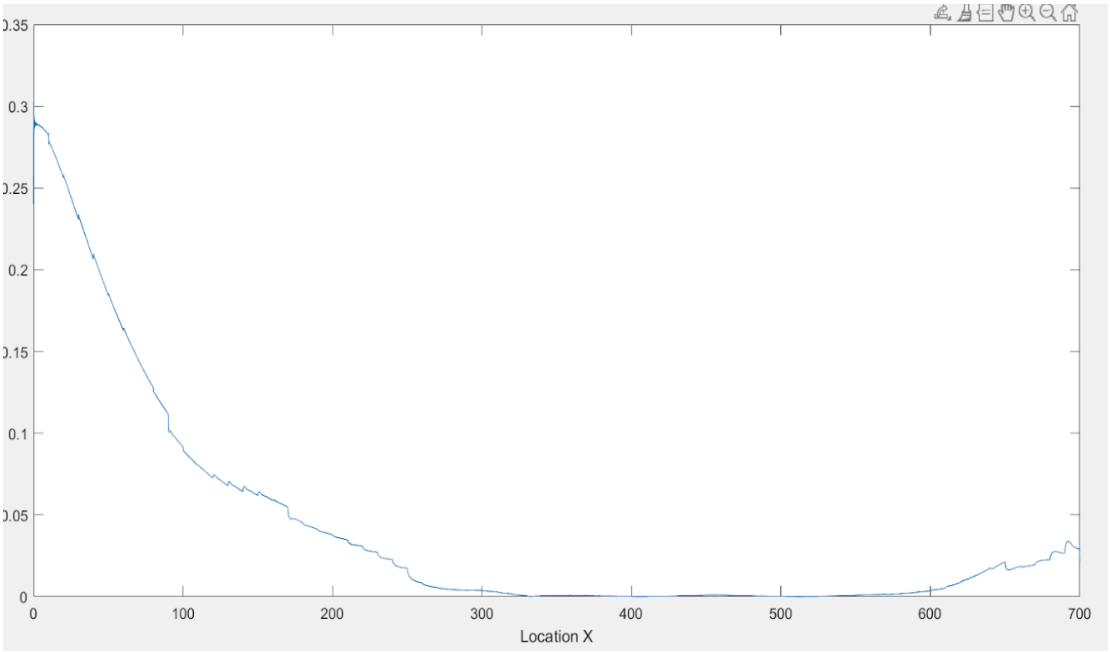

Figure 3 Surface Current Plot from EFIE

4.2 Parallelization Method Result

The total groups as per in the fast method is 13, the observation point is raised to 2.4 metres. Various values were tried for the two and these vales seemed to give the closest results as that of the EFIE. The terrain profile is further divided into n-arbitrary segments, in the context of the project in the end the calculated number of the segments was 697. Propagation and scattering happens from the transmitter and each segment. The calculation of the electric field is done in parallel.

Here, the parallelization method has been used with the above stated fast method and the earlier EFIE. Different results have been presented.

a. Parallelization method using the original fast method.

The following plot depicts the surface current using this method.

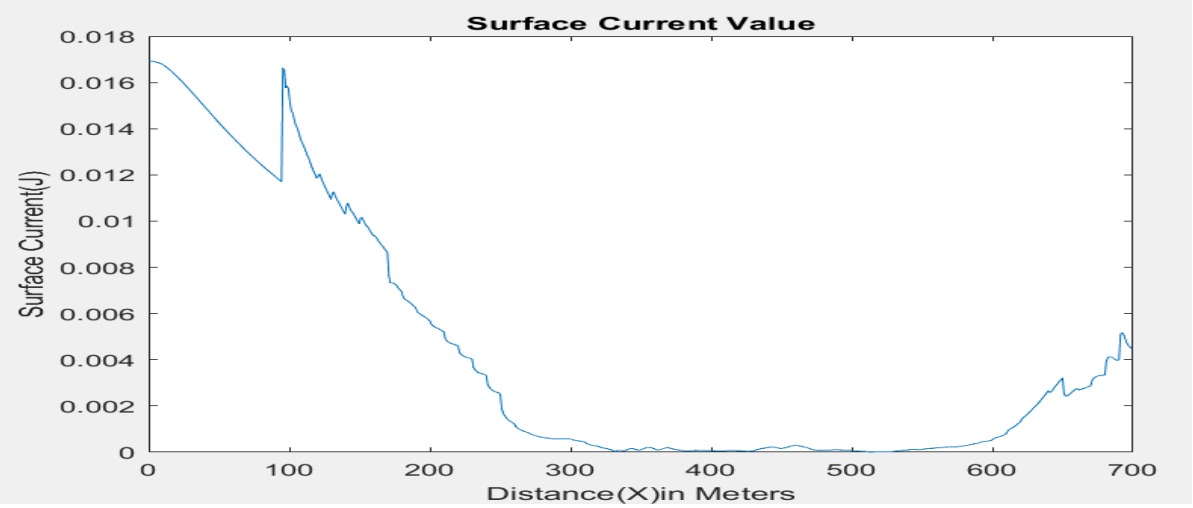

Figure 4 Surface current plot from parallelization using Fast method

The graph is pretty close to EFIE even though there is an anamoly in around 100 metres as the graph rises up. This is probably because in parallel calculation, the scattered rays add upto the incident ray after the first hundred metres segment more strongly and signal starts fading later on.

The following is the plot for the parallelization method derived electric field using the fast method. Now the plot is not bad but definitely not as similar to the EFIE one as it should be. It is further discussed in the 'future work' section below.

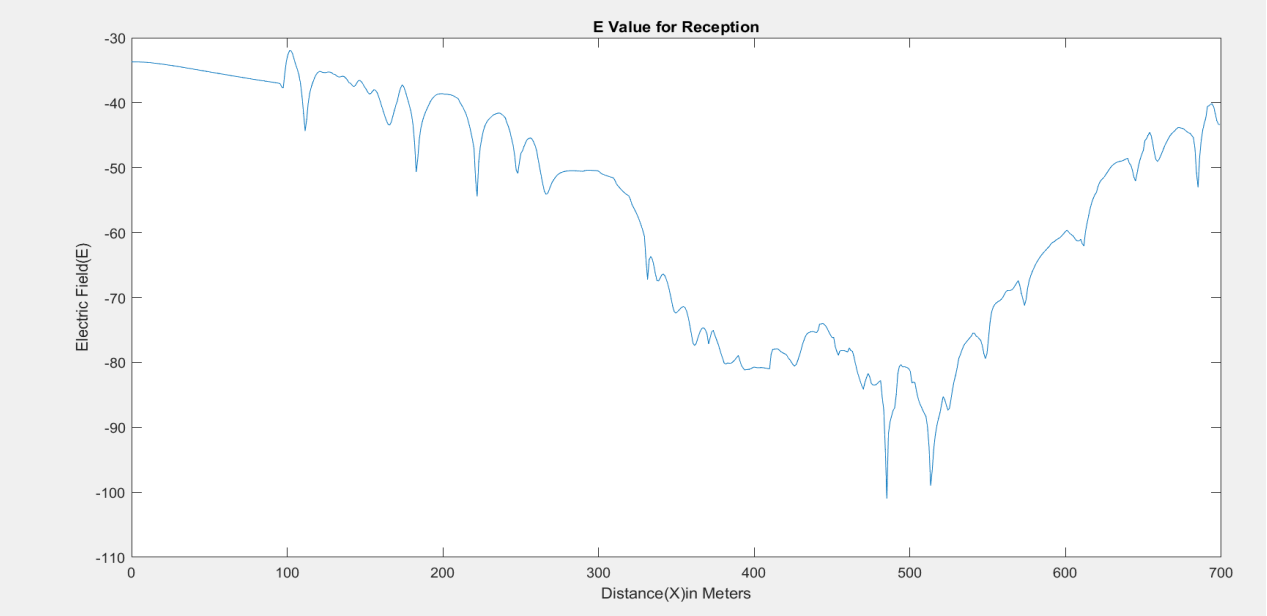

Figure 5 E vs Distance plot from parallelization using Fast method

b. Parallelization method using the earlier EFIE.

Using the parallelisation method with the earlier EFIE method (Absence of bifurcation of groups) gives a slightly different result as compared to using it with the faster method. The plots here are actually more similar to the EFIE and gives desired results, however, do not fulfil the time complexities problem much. Even though faster than just the EFIE, this method still takes a reasonable time to execute.

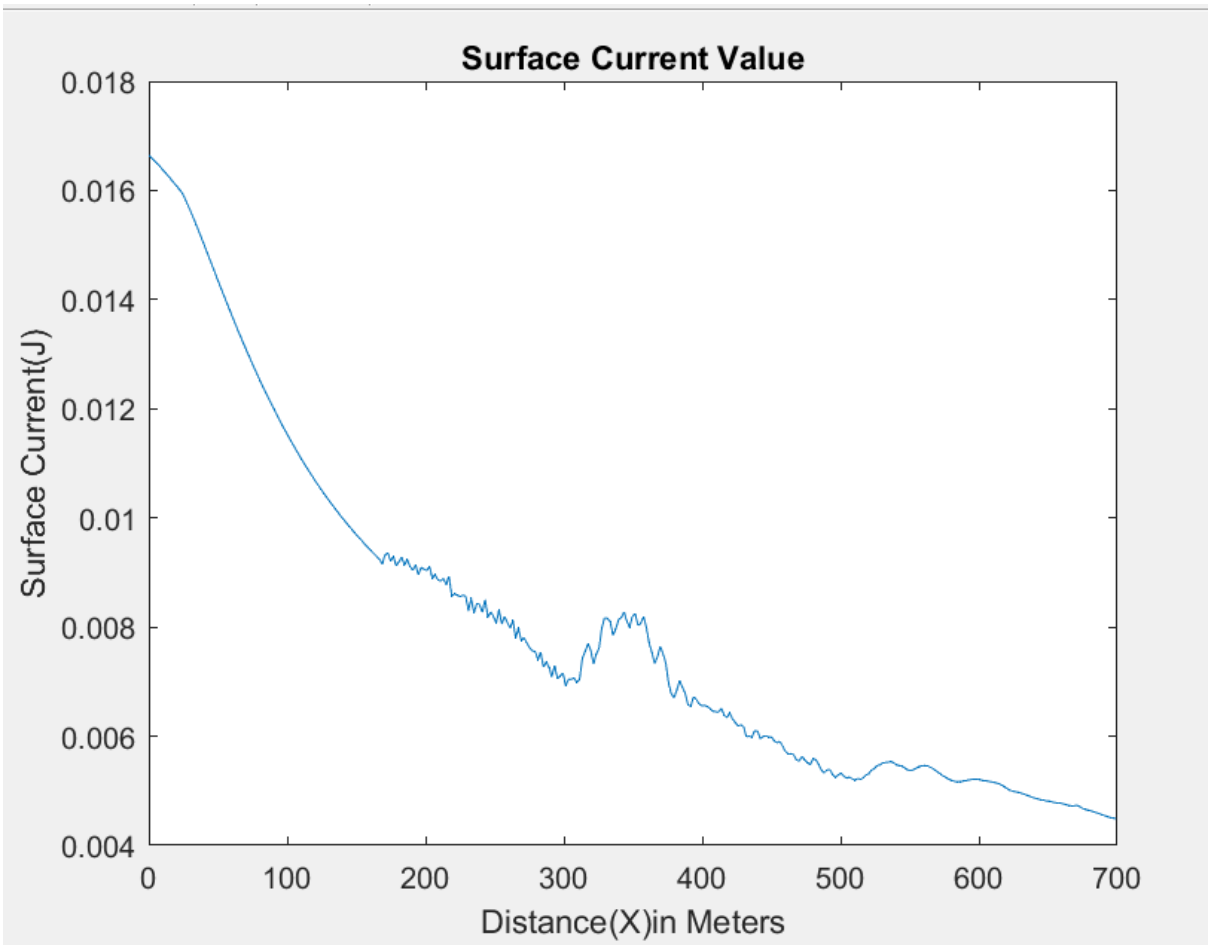

Figure 6 Surface Current vs Distance (Parallelization with traditional EFIE method)

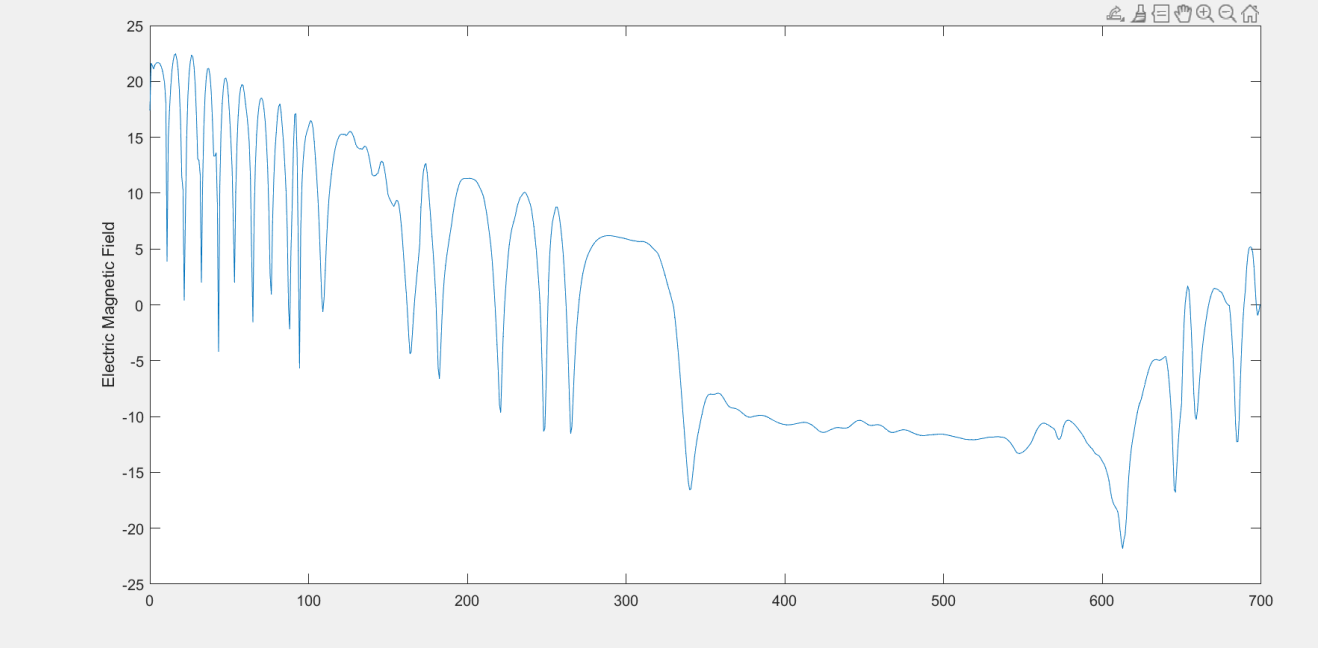

Figure 7 E vs Distance (Parallelization with traditional EFIE method)

4.3 Results of Time

Now, as the hypothesis suggests, the parallelization method should be faster than the traditional EFIE method. Below are the time comparisons for the same.

As seen below, the time for execution for each division of distance with a 100 metres interval is given below. The parallelization method is at least 2000 times faster than the EFIE method.

Distance	EFIE Time Taken	Parallelization Time Taken
700	8988	4.06
600	7440	3.48
500	6420	2.9
400	5136	2.32
300	3852	1.74
200	2568	1.16
100	1284	0.58

Figure 8 Time comparisons

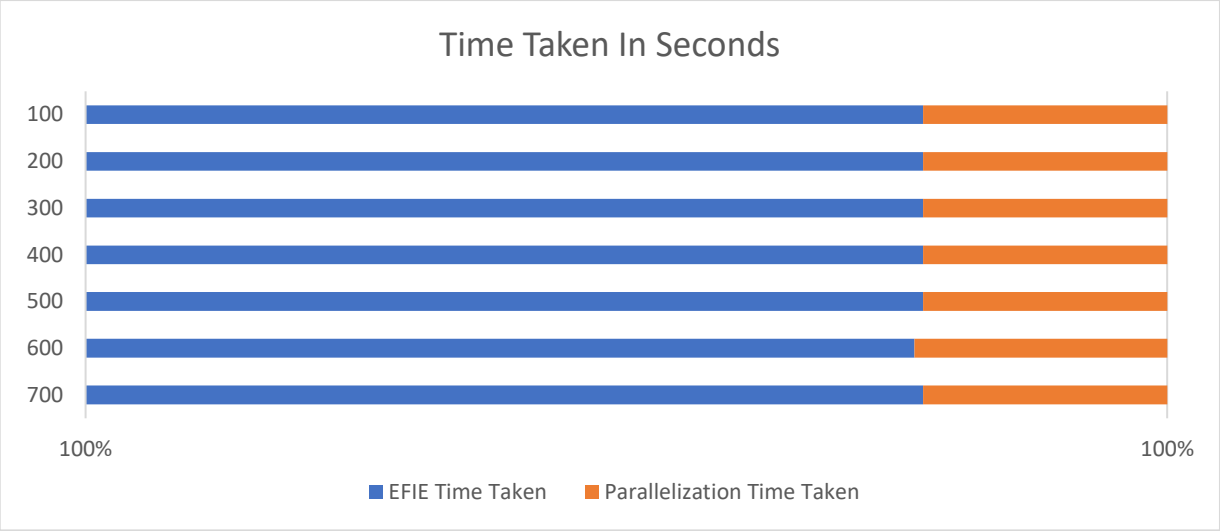

Figure 9 Time comparison plot

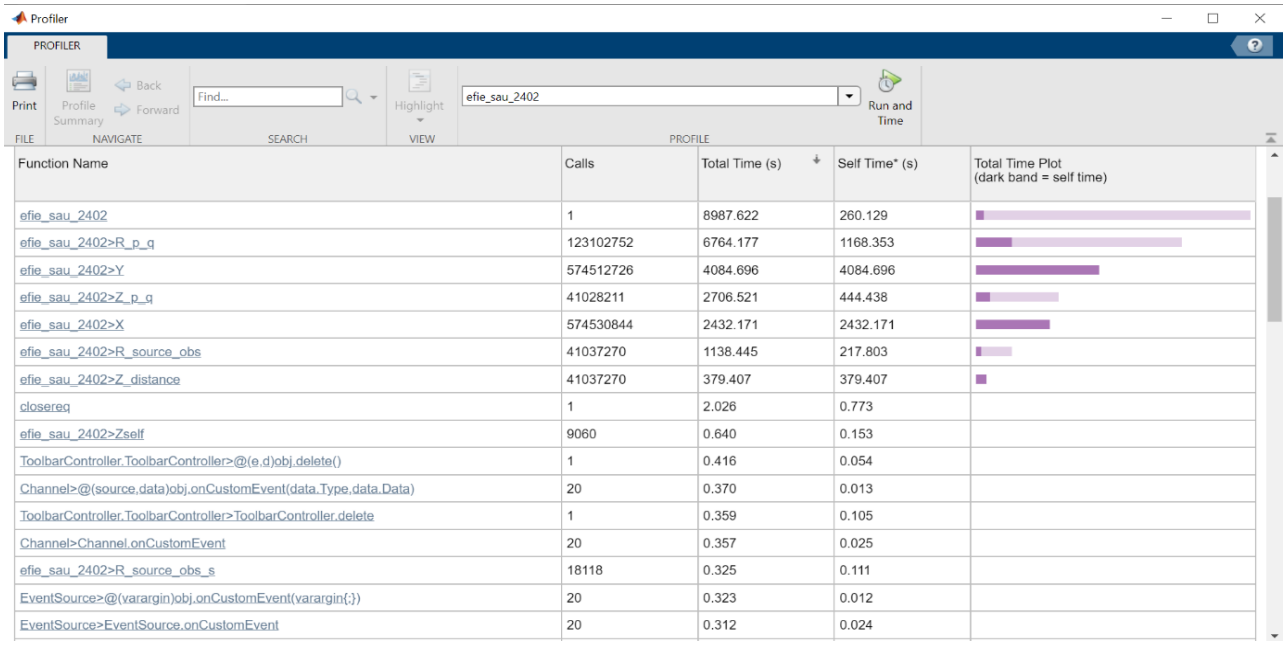

Function Name	Calls	Total Time (s)	Self Time* (s)	Total Time Plot (dark band = self time)
efie_sau_2402	1	8987.622	260.129	
efie_sau_2402>R_p_q	123102752	6764.177	1168.353	
efie_sau_2402>Y	574512726	4084.696	4084.696	
efie_sau_2402>Z_p_q	41028211	2706.521	444.438	
efie_sau_2402>X	574530844	2432.171	2432.171	
efie_sau_2402>R_source_obs	41037270	1138.445	217.803	
efie_sau_2402>Z_distance	41037270	379.407	379.407	
closereq	1	2.026	0.773	
efie_sau_2402>Zself	9060	0.640	0.153	
ToolbarController.ToolbarController>@(e,d)obj.delete()	1	0.416	0.054	
Channel>@(source,data)obj.onCustomEvent(data.Type,data.Data)	20	0.370	0.013	
ToolbarController.ToolbarController>ToolbarController.delete	1	0.359	0.105	
Channel>Channel.onCustomEvent	20	0.357	0.025	
efie_sau_2402>R_source_obs_s	18118	0.325	0.111	
EventSource>@(varargin)obj.onCustomEvent(varargin{:})	20	0.323	0.012	
EventSource>EventSource.onCustomEvent	20	0.312	0.024	

Figure 10 Time recording of EFIE execution in MATLAB

Function Name	Calls	Total Time (s)	Self Time* (s)	Total Time Plot (dark band = self time)
EFIE	1	4.600	0.641	
EFIE>R_surface_obs	181503	1.565	0.560	
EFIE>R_p_q	181503	1.559	0.539	
EFIE>Y	728103	1.503	1.027	
EFIE>X	1457600	1.014	1.014	
EFIE>H02	364412	0.537	0.537	
newplotwrapper	2	0.214	0.007	
newplot	2	0.208	0.023	
CanvasPlugin.CanvasPlugin>CanvasPlugin.createCanvas	2	0.114	0.009	
UnifiedAxesInteractions>UnifiedAxesInteractions.createDefaultInteractions	2	0.083	0.026	
CanvasSetup>CanvasSetup.createScribeLayers	2	0.069	0.006	
ScribeStackManager.ScribeStackManager>ScribeStackManager.getLayer	8	0.064	0.011	
ScribeStackManager.ScribeStackManager>ScribeStackManager.createLayer	6	0.047	0.008	
UnifiedAxesInteractions>UnifiedAxesInteractions.createInteractionsForTitlesAndLabels	2	0.046	0.001	
UnifiedAxesInteractions>UnifiedAxesInteractions.createCartesianAxesTextInteractions	2	0.045	0.002	
UnifiedAxesInteractions>UnifiedAxesInteractions.setDefaultBehaviorForTextArray	2	0.043	0.002	

Figure 11 Time recording of Parallelization execution in MATLAB

4.4 Okumura Hata Model

A graphical path loss (PL) data empirical formulation is the Hata model. It is effective between 150 MHz and 1500 MHz, ours is 960 so goes well. Its name comes from the fact that Okumura provides it. Hata provided a common formula for propagation loss in an urban setting. For other scenarios, he has also offered correction formulae. Some formulas and steps are obtained from the internet and hard coded it to understand the path loss. There are different formulae for different types of terrain environment.

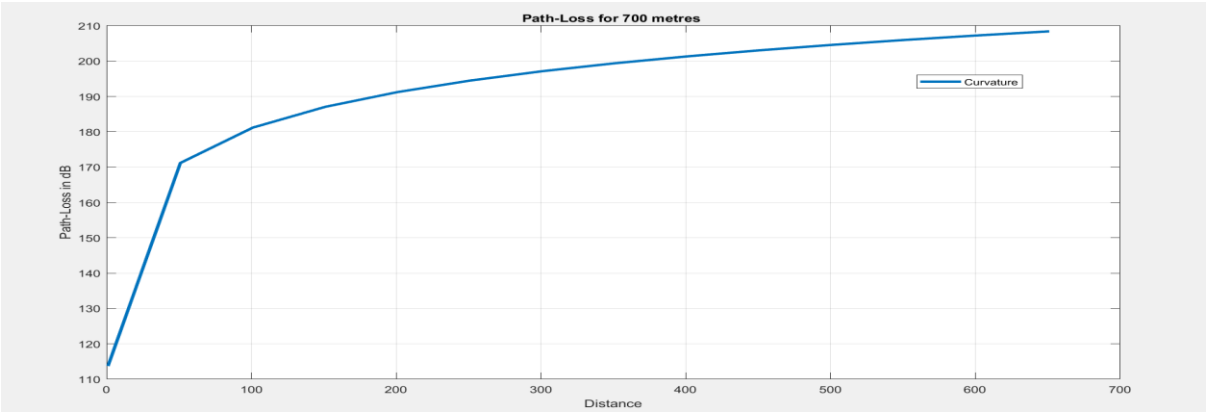

Figure 12 Okumura Hata Model (700 km span)

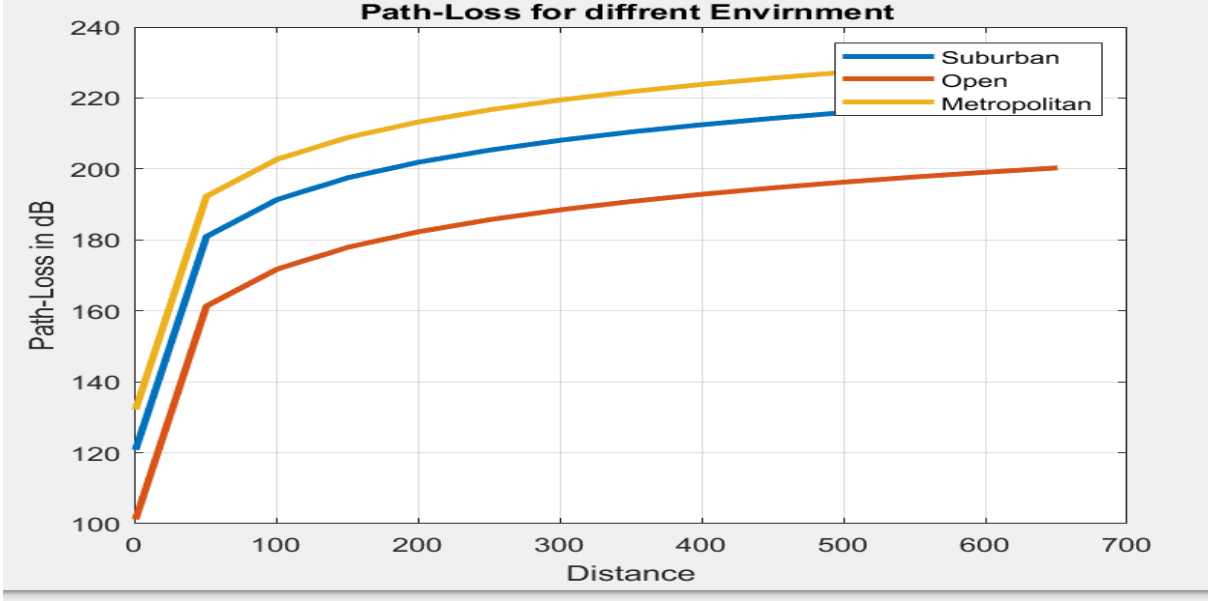

Figure 13 Okumura Hata Model (700 km span for different environments)

4.5 Limitations

The study has some limitations and as it is clear by the graphs there are some anomalies involved.

a. The terrain span ranges up to 700 metres only.
b. The graph isn't properly equivalent to the traditional EFIE-obtained graph, especially with the fast method despite a lot of brainstorming, trials and tribulations. This might be due to the inability to incorporate backward scattering in fast method, though not necessarily too. Due to time constraints of the thesis, the part could not be taken care of properly.
c. The Okumura Hata model has not been implemented for the given terrain profile data set.
d. Only forward scattering has been taken into account for the parallelization with fast method. This is due to the author's inability to take backscattering into account.

Chapter 5: Conclusion

The signal propagation on a data set using the parallelization approach which was built in the previous chapter was tested, and it was shown how this confirms the theory. The parallelization method was based on the 2012 paper 'Parallel Recursive Implementation of EFIE for Arbitrary Terrain Profile' referenced at (Delaney, et al., 2011). The 2008 paper (Nuallain, 2008) served as the basis for this and the results obtained were satisfactory holding conformity to the base paper. This chapter provides a summary of the project and its findings as well as discussion of the next steps.

5.1 Project Overview

One of the many techniques used to determine how communication signals will spread, including ray tracing and integral methods is the Electric Field Integration Equation (EFIE). Since the EFIE established a relationship, it was possible to calculate the electric field E that an electric current produces (J). A terrain profile and the equation E=ZJ are available. Taking this, the goal of this project is to identify practical solutions that will speed up the process of graphically determining the signal coverage for every terrain profile.

A more efficient technique for doing this, known as the parallelization approach, is also described. In this method, computation is carried out on bifurcated terrain groups and segments.

It is set off until 700 metres from the transmitter. The viewing point is raised to 2.4 meters, and there are a total of 13 groups according to the quick method. Different values were explored for the two, and these values appeared to produce outcomes that were most similar to those of the EFIE. In the context of the project, the determined total number of segments was 697. The terrain profile is further divided into n-arbitrary segments. Each segment and the transmitter both experience propagation and scattering. The electric field is calculated simultaneously in parallel.

5.2 Contribution

The signal coverage study becomes faster and more efficient. This method is almost 2000 times faster than the traditional EFIE method. Additionally, this may pave the way for more fruitful study into the cognitive radio technology. Cognitive radios (CRs) analyse a supported network architecture for each transmission request. The network server either accepts or rejects these requests based on its assessment of the transmission's likely effects on participants and other CR devices given the CR's geo-location and antenna properties

5.3 Future Work

Likewise, many such ideas can be thought of for faster implementation of the Electric Field Integration Equation. Due to time constraints, the anomaly on the plot (particularly for the first 100 metres) could not be solved and the Okumura- Hata model was not implemented with the given terrain profile data set. These make lots of work that can be carried out in the future. Further, the backscattering approximation can be taken into account in the parallelization method used with the fast method so that it can be done properly and more effectively.

References

Alavi, R. R., Mirzavand, R., Doucette, J. & Mousavi, P., 2020. *Fast Source Reconstruction Method in Near-Field to Far-Field Transformation Algorithm,* Montreal: IEEE.

Ashikhmin, A., Li, L. & Marzetta, T. L., 2018. Interference Reduction in Multi-Cell Massive MIMO Systems With Large-Scale Fading Precoding. *IEEE Transactions on Information Theory,* 64(9), pp. 6340-6361.

Delaney, J., Feng, Z. & O'Nuallain, E., 2011. *Parallel Recursive Implementation of EFIE for Arbitrary Terrain Profile,* Dublin: Trinity College Dublin.

El-Gohnary, H., 2011. *International Journal of Interdisciplinary Telecommunications and Networking.* 3rd ed. s.l.:IGI Global.

Fette, B., 2006. *Cognitive Radio Technology.* Burlibgton: Elsevier Publication.

Kayode, A., Ogunremi, O. K. & Ojedokun, I. A., 2016. Optimization of Okumura-Hata Model for Long Term Evolution Network Deployment in Lagos, Nigeria. *International Journal on Communications Antenna and Propagation (IRECAP),* pp. 146-152.

Mahmood, T., Mohamed, W. Q. & Imran, O. A., 2021. *Factors Influencing the Shadow Path Loss Model with Different Antenna Gains Over Large-Scale Fading Channel.* Bandung, IEEE, pp. 1-5.

Nuallain, E. O., 2008. *A Proposed Propagation-based Methodology with which to address the Hidden Node Problem and Security/Reliability Issues in Cognitive Radio,* Dublin: IEEE.

Saunders, S. R. & Zavala, . A., 2007. *Antennas and Propagation for Wireless Communication System.* West Sussex: John Wiley & Sons Ltd.

Shi, Y. et al., 2010. *A stable marching-on-in-time solver for time domain surface electric field integral equations based on exact integration technique.* Toronto, IEEE, pp. 1-4.

Si, D., Wang, J., Wei, G. & Yan, X., 2019. Method and Experimental Study of Voltage Measurement Based on Electric Field Integral With Gauss–Legendre Algorithm. *IEEE Transactions on Instrumentation and Measurement,* pp. 2771 - 2778.

Appendix

Please find my code in the following repository in GitHub:

https://github.com/saubhagyasharma99/Dissertation_Parallelisation-